Progress In Electromagnetics Research M, Vol. 20, 13–27, 2011

A NOVEL DESIGN OF MODIFIED COMPOSITE RIGHT/LEFT-HANDED UNIT CELL

S. Ramezanpour*, S. Nikmehr, and A. Poorziad

Faculty of Electrical and Computer Engineering, University of Tabriz, 29 Bahman Boulevard, Tabriz, Iran

Abstract—Design procedure for a modified Composite Right/Left Handed (CRLH) unit cell is represented. The ferroelectric interdigital capacitor (IDC) is used as a tuned capacitor, and spiral inductor is utilized to implement inductors. A modified CRLH unit cell is attained by moving the shunt inductor of conventional unit cell to both ends with doubled values. In this manner, only one bias network would be required for each unit cell. The parameters of the designed unit cell are obtained so that the Bloch impedance to be equal to 50 Ω and the Bloch propagation constant to have one zero at the operational frequency. The operational frequency is chosen equal to 11.45 GHz, which is in the Ku-band and in middle of the up-link satellite communications. To design the modified unit cell, initially, the unit cell without a shunt capacitor is constructed. This would result in Π-model structure for which the element dimensions are varied to reach the desired values. Next, the shunt capacitor is added to the model and its length is varied until the balanced condition is achieved.

1. INTRODUCTION

The theory of CRLH metamaterials describes dual right-handed (RH)/left-handed (LH) nature of metamaterials. The continuous transition from LH to RH, in the dispersion curve of a CRLH metamaterial (MTM), is called the balanced condition. The periodic structure of CRLH unit cells in the balanced condition leads to a CRLH leaky-wave antenna (LWA) [1]. The CRLH transmission line can also be bent into a circle to realize a ring antenna [2].

A CRLH unit cell can be realized by incorporating lumped or distributed elements in series and parallel branches. However, in [3]

Received 7 July 2011, Accepted 28 July 2011, Scheduled 7 August 2011

* Corresponding author: Shahab Ramezanpour (shahabramezanpour@yahoo.com).

it is constructed by coupled lines with slotted ground. The number of right-handed or left-handed frequency bands can be increased with higher order unit cell [4]. Use of wire bonded interdigital capacitor (WBIDC) in the CRLH unit-cell improves high frequency performance by reducing undesired self resonances generated in IDC at lower frequency end which leads to reach wider frequency band [5, 6]. In [7], A CRLH unit cell composed with arbitrarily adjustable lumped-elements is designed in a dual metal-plane configuration in order to construct a filter with wide fractional bandwidth. In [8], Composite right/left-handed (CRLH) substrate integrated waveguide (SIW) and half mode substrate integrated waveguide (HMSIW) leaky-wave structures for antenna applications are proposed and investigated. SIW and HMSIW are popular types of planar guided-wave structures which have desirable features such as low profile, low cost, and easy integration with planar circuits.

A CRLH LWA provides full-space scanning capability. It is a frequency dependent structure, however modern communication systems, generally require fixed frequency operation. The propagation constant, β, in CRLH transmission lines vary with both frequency and LC parameters. Tuning LC parameters at a fixed frequency can be obtained by incorporating varactor diodes [9] and/or tunable inductor chips [10] along the structure. It is also possible to use ferrite components to obtain a tuned inductor and ferroelectrics for a tuned capacitor. Ferrites and ferroelectrics may be used either in bulk materials or thin films. The latter case is compatible with monolithic integrated circuit (MIC) technology [11]. In comparison with varactor diodes, variable capacitors using thin film ferroelectric materials have low cost, high speed and integration capability with MICs [12]. Tunable capacitors using thin film ferroelectric, have two conventional structures; parallel plates (metal-insulator-metal (MIM)) and interdigital capacitors (IDC). IDC varactors require higher tuning voltage compared to MIMs, therefore, they are less sensitive to AC voltages. In addition, unlike MIMs, they require only one level of metallization [13].

In this paper, an interdigital capacitor with thin film ferroelectric is used as a tuned capacitor and spiral inductor is used to implement inductors. The unit cell is designed in a CPW configuration in which the ground plane and signal strips are formed on one side of the substrate [14, 15]. The designed unit cell has a very compact size and is compatible with MIC technology, because it is designed in coplanar structure and also a thin film ferroelectric layer is utilized underneath the IDCs to be as tuned elements. In conventional CRLH unit cell the parallel capacitor (and also series inductor) acts as a

parasitic element. However, in our modified unit cell it is created by a separate IDC, therefore we can have tuned elements in both series and parallel branches which leads to maintaining the characteristic impedance almost constant by varying tuned capacitors. Furthermore, the designed unit cell has arbitrarily controllable response due to the independently adjustable element values.

2. CONVENTIONAL CRLH UNIT CELL

The circuit model of a CRLH unit cell is depicted in Fig. 1(a). A typical CRLH Bloch dispersion relation, $\beta_B(\omega)$ is plotted in Fig. 1(b). In the balanced condition the series and shunt resonances (ω_1 and ω_2) are equal which leads to a continuous transition between LH band ($\beta < 0$) and RH band ($\beta > 0$) (Fig. 1(c)) [1]. In the balanced condition:

$$\omega_1 = \omega_2 = \omega_0 \tag{1}$$

where, $\omega_1 = \frac{1}{\sqrt{ab}}$, $\omega_2 = \frac{1}{\sqrt{cd}}$ and ω_0 is the operational or transition frequency.

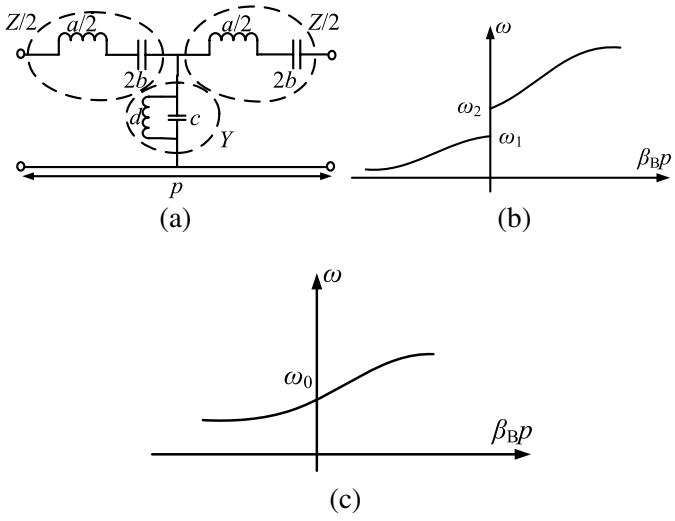

Figure 1. (a) Circuit model of a CRLH TL unit cell. (b) Typical CRLH Bloch dispersion diagram. (c) Bloch dispersion diagram in the balanced condition.

3. MODIFIED CRLH UNIT CELL

3.1. Circuit Model and Parameter Definition

Using tuned elements to vary propagation constant, would also change the characteristic impedance. To maintain characteristic impedance almost constant, tuned elements (ferroelectric IDCs) are used in both series and shunt branches. For using only one bias network for each unit cell, the shunt inductor from conventional CRLH unit cell is moved to the both ends with a value which is multiplied by two [9]. The resultant configuration is shown in Fig. 2. A unit cell is characterised by Bloch parameters, i.e., the Bloch propagation constant and Bloch impedance. Bloch parameters can be determined from $ABCD$ parameters of the circuit [16]. For a reciprocal and symmetrical unit cell:

$$Z_B = \frac{\pm B}{\sqrt{A^2 - 1}}, \quad \cosh(\gamma_B p) = \frac{A + D}{2} \tag{2}$$

Considering $\gamma_B = j\beta_B$, $AD - BC = 1$ and $A = D$, Eq. (2) is modified to:

$$Z_B = \sqrt{\frac{B}{C}}, \quad \cos(\beta_B p) = A \tag{3}$$

$ABCD$ parameters are converted to S-parameters by the relations:

$$\begin{aligned} A &= \frac{1 - S_{11}^2 + S_{12}^2}{2S_{12}}, \quad B = Z_0 \frac{(1 + S_{11})^2 - S_{12}^2}{2S_{12}}, \\ C &= \frac{1}{Z_0} \frac{(1 - S_{11})^2 - S_{12}^2}{2S_{12}} \end{aligned} \tag{4}$$

Substituting Eq. (4) into (3) yields:

$$Z_B = Z_0 \sqrt{\frac{(1 + S_{11})^2 - S_{12}^2}{(1 - S_{11})^2 - S_{12}^2}} \quad ; \quad \beta_B p = \arccos\left(\frac{1 - S_{11}^2 + S_{12}^2}{2S_{12}}\right) \tag{5}$$

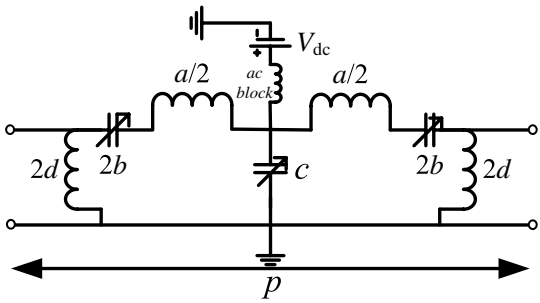

Figure 2. Circuit model of the modified CRLH unit cell.

The unknown parameters a, b, c and d of the circuit model of Fig. 2 are determined so that the operational frequency has the value of 11.45 GHz. The frequency of 11.45 GHz is in the Ku-band and in middle of the up-link satellite communication band (11.2–11.7 GHz) [17]. Also, we must have the balanced condition, i.e., the condition that the Bloch propagation constant, β_B, have one zero at transition (operational) frequency and the Bloch impedance, Z_B, have a flat diagram and be equal to 50 Ω at this frequency. The resultant parameters called set I parameters, are shown in Table 1.

Table 1. Values of the elements of the unit cell.

	a (nH)	b (pF)	c (pF)	$2d$ (nH)	L_c (nH)	C_c (pF)	L_{2d} (nH)	C_{2d} (pF)
set I	1.38	0.14	0.33	1.18	-	-	-	-
set II	1.38	0.14	-	-	0.1	0.28	1.01	0.027

3.2. Element Implementation

To implement elements, ferroelectric IDC is used for capacitors and spiral inductor for inductors. Fig. 3 shows the layout of an IDC and a spiral inductor. For IDC, the quantities $2s$, $2g$, $2g_e$, ℓ, $2w$, and n stand for finger width, gap between fingers, gap at end of fingers, overlapping length, electrode width and number of fingers, respectively. For the spiral inductor, the parameters ℓ_1, ℓ_2, w, s, and n are, respectively, length of first outermost segment, length of second outermost segment, conductor width, conductor spacing, and number of turns. To determine the scattering parameters and de-embedding, a short section of microstrip TL is added at each end of the components [11].

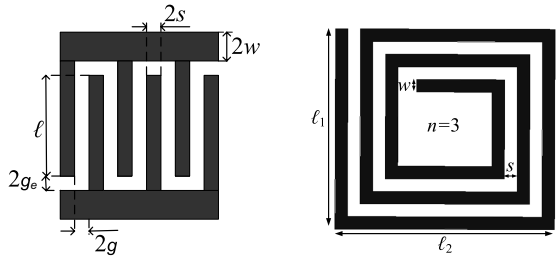

Figure 3. (a) Layout of an IDC. (b) Layout of a spiral inductor.

Two CPW lines, one with strips of width 16 μm (for simulation of the structures except series IDC and unit cell) and another with strips of width 68 μm (for simulation of series IDC and unit cell) are utilized in this paper. All simulation results are obtained by Ansoft HFSS simulator. Characteristic impedance and propagation constant of these two lines are depicted in Fig. 4. The gap between strips is varied until the characteristic impedance attains the value of 50 Ω.

An IDC can be modelled with a series capacitor, series inductor and parallel capacitors (Fig. 5). This is a Π-model of the structure

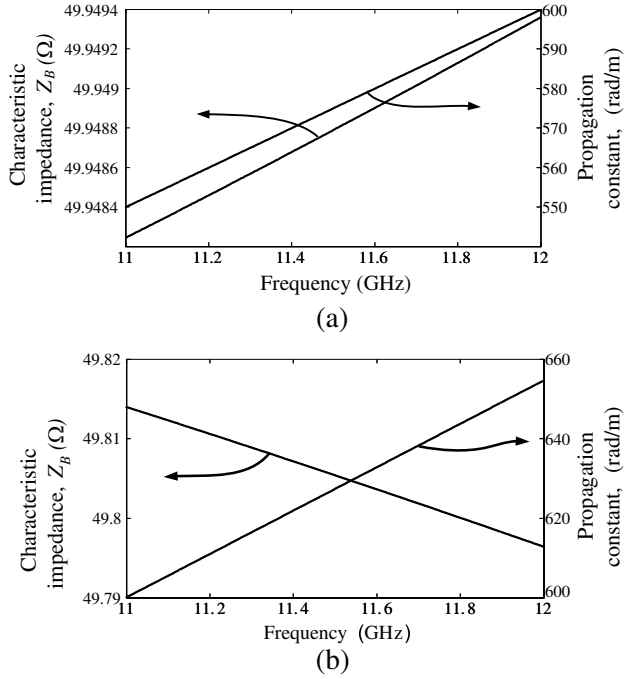

Figure 4. Propagation constant and characteristic impedance of CPW lines. (a) CPW line with strips of width 16 μm and gaps 9 μm. (b) CPW line with strips of width 68 μm and gaps 29 μm.

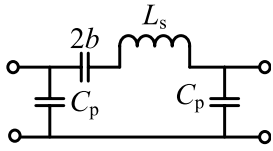

Figure 5. Circuit model of an IDC.

and its elements can be related to Y-parameters of the circuit model. The relation of the series capacitor and inductor with Y-parameters are [11]:

$$2b = \frac{2}{j\omega} \frac{1}{\omega \frac{d}{d\omega}\left(Y_{12d}^{-1}\right) - Y_{12d}^{-1}} \quad ; \quad L_s = \frac{-1}{j2\omega}\left(\omega \frac{d}{d\omega}\left(Y_{12d}^{-1}\right) + Y_{12d}^{-1}\right) \quad (6)$$

Y_{11d} and Y_{12d} are the de-embedded Y-parameters which is obtained from de-embedded S-parameters.

We consider the following quantities for the structure: permittivity of ferroelectric layer, $\varepsilon_2 = 256$, permittivity of the substrate, $\varepsilon_1 = 9.8$, thickness of ferroelectric layer, $h_2 = 2\,\mu\text{m}$ and thickness of the substrate layer, $h_1 = 200\,\mu\text{m}$. Then, using the conformal mapping method as in [18], parameters of the series ferroelectric IDC with $2b = 0.28$ are obtained as: $2s = 2g_e = 2w = 8\,\mu\text{m}$, $2g = 4\,\mu\text{m}$, $\ell = 57\,\mu\text{m}$, $n = 6$.

For simulation, these parameters are used as initial values and the length of IDC is varied to reach the desired value of $2b = 0.28\,\text{pF}$. Fig. 6(a) shows the simulation results of IDC in which $2b$ and L_s are obtained from (6).

With the value of L_s at 11.45 GHz from Fig. 6(a), the required inductor in series branch of unit cell can be found from:

$$L_r = \frac{a}{2} - L_s = 0.61\,\text{nH} \quad (7)$$

L_r, c and $2d$ are also demonstrated in Figs. 6(b) and (c). For these elements, the values of capacitor and inductors can be obtained from the following equations.

$$C = -\frac{Y_{12d}}{j\omega}, \quad L = -\frac{1}{j\omega Y_{12d}} \quad (8)$$

An IDC is utilized to implement parallel capacitor but as mentioned it is comprised of a series capacitor and inductor. However, to construct the unit cell, first, it is modelled by a single capacitor as the equivalent capacitor and designed so that to obtain the value $c = 0.33\,\text{pF}$, then, in the circuit model, it is replaced with the mentioned series capacitor and inductor.

The dimensions of each individual element was determined and are given in Table 2 with subscript i.

3.3. Π-model Structure

In the previous section, the procedure of determining the dimensions of individual elements was explained. To confirm the accuracy of these dimensions, it is necessary to determine them when they are placed

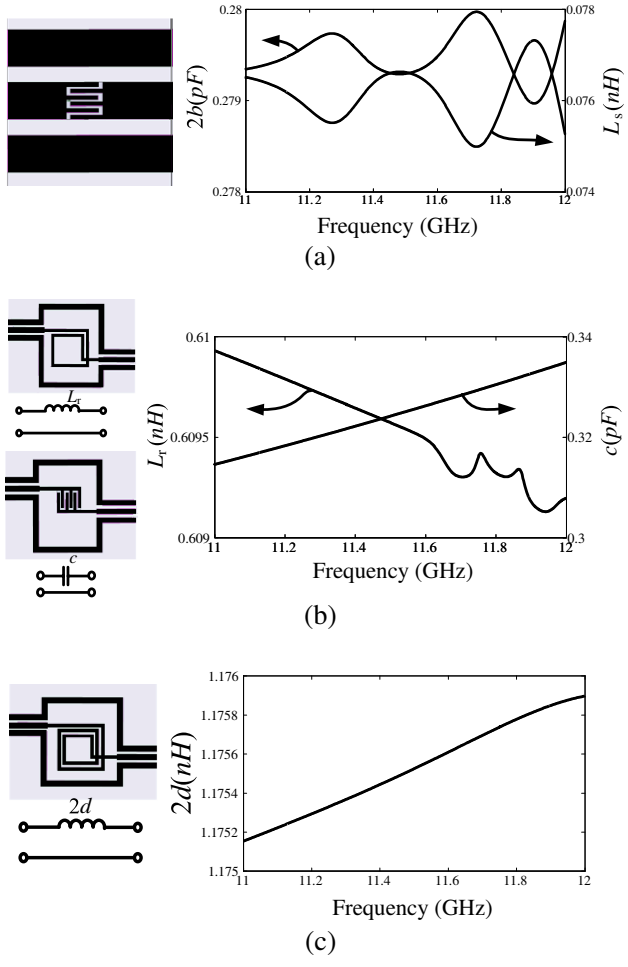

Figure 6. (a) Series capacitor: $2b$ and L_s. (b) Series inductor and parallel capacitor: L_r and c. (c) Parallel inductor: $2d$.

in unit cell configuration. To relate the element values to Y or Z parameters of the circuit model, it should be converted to Π or T models, respectively. For Π-model, the parallel capacitor is removed from the unit cell (Fig. 7) and the elements values are determined from,

$$\begin{aligned} a &= -\frac{1}{j2\omega}\left(\omega\frac{d}{d\omega}(Y_{12d}^{-1}) + Y_{12d}^{-1}\right) \\ b &= \frac{2}{j\omega}\frac{1}{\left(\omega\frac{d}{d\omega}(Y_{12d}^{-1}) - Y_{12d}^{-1}\right)}\ ,\ 2d = \frac{1}{j\omega(Y_{11d}+Y_{12d})} \end{aligned} \tag{9}$$

Table 2. Comparison of the elements dimensions.

		$2b_i$	$2b_u$	c_i	c_u
capacitors	$2s$ (μm)	8	8	8	8
	$2g$ (μm)	4	4	4	4
	$2g_e$ (μm)	8	8	8	8
	$2w$ (μm)	8	8	8	8
	ℓ (μm)	51	48	42	33
	n	6	6	6	6
		L_{ri}	L_{ru}	$2d_i$	$2d_u$
inductors	ℓ_1 (μm)	121	121	139	127
	ℓ_2 (μm)	121	121	139	127
	w (μm)	8	8	8	8
	s (μm)	8	8	8	8
	n	1.5	1.5	2.5	2.5

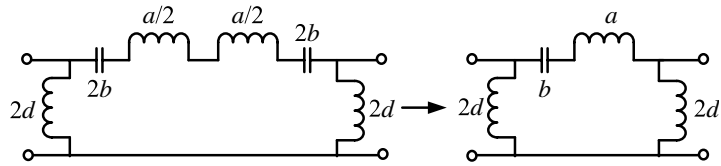

Figure 7. Circuit model of the unit cell without parallel capacitor.

The elements which was designed individually are used in the Π-model structure and their dimensions are varied until the desired quantities of parameters set I are achieved. The unit cell without parallel capacitor and its elements values are depicted in Fig. 8.

3.4. Final Design of the Unit Cell

To complete our unit cell design, the parallel capacitor which was previously designed is added to Π-model structure and its length is varied until the balanced condition is achieved (i.e., the condition that β_B have one zero at transition frequency and Z_B have a flat diagram at this frequency). The designed unit cell is shown in Fig. 9(a). The simulation results of Z_B and β are depicted in Figs. 9(b) and (c) (Z_B and β are obtained from Eq. (5)).

Metamaterial transmission line can be created by cascading the designed unit cells such that two parallel inductors with value of $2d$

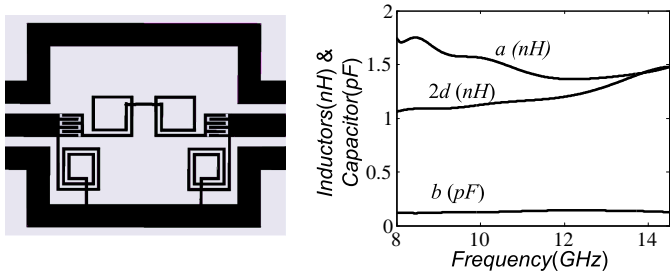

Figure 8. (a) Π-model structure. (b) Diagrams of the values of the elements.

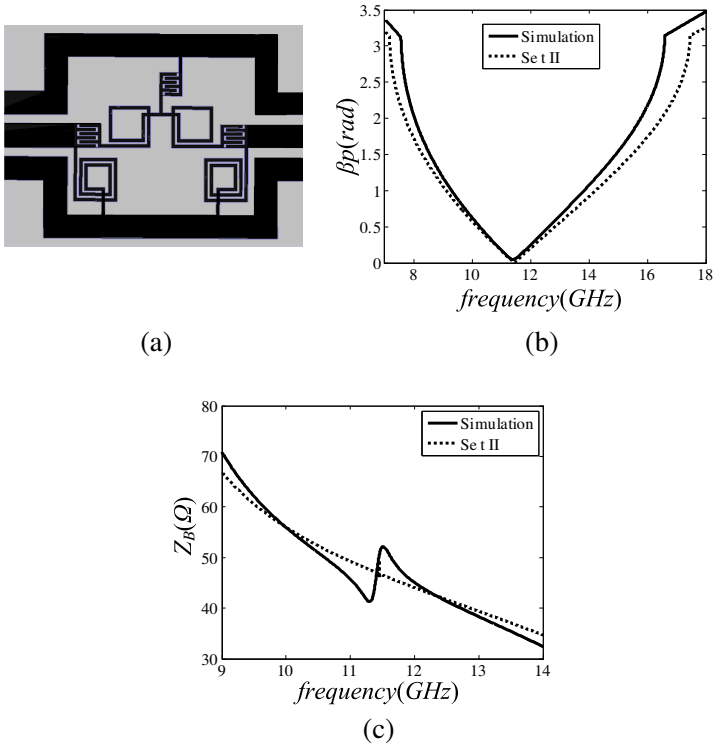

Figure 9. Designed unit cell and Bloch equivalents obtained from circuit model using set II parameters and simulation. (a) Designed unit cell. (b) Bloch propagation constant. (c) Bloch impedance.

which are created at the connections, can be replaced by one with value of d.

3.5. Comparison of the Elements Dimensions

Table 2 compares dimensions of the elements which are obtained individually (with subscript i) with those of elements which are inserted in unit cell configuration (with subscript u).

Scrutiny of this table demonstrates that the series elements are well matched but not the parallel elements. This is due to ignoring the coupling effects of the parallel inductors with ground strips. Since the dimensions of parallel inductors obtained individually and in the unit cell configuration are not identical, therefore, the dimensions of parallel capacitor which resonates with parallel inductors at operational frequency is not identical, as well.

3.6. Parasitic Elements of the Parallel Elements

3.6.1. Parallel IDC

We have modelled the parallel IDC with a single capacitor (c), but in fact it is comprised of a series capacitor (C_c) and a series inductor (L_c). The quantity $c = 0.33\,\text{pF}$ is related to the equivalent capacitance by:

$$\frac{1}{j\omega c} = j\omega L_c + \frac{1}{j\omega C_c} \tag{10}$$

To determine L_c and C_c, the parallel inductors of the unit cell is removed from the configuration, which results in a T-model (Fig. 10). In this structure L_c and C_c are determined from Z-parameters as:

$$L_c = \frac{1}{j2\omega}\left(Z_{12d} + \omega\frac{d}{d\omega}(Z_{12d})\right) \quad ; \quad C_c = \frac{2}{j\omega}\frac{1}{Z_{12d} - \omega\frac{d}{d\omega}(Z_{12d})} \tag{11}$$

Z_{11d} and Z_{12d} are de-embedded Z-parameters which are obtained from de-embedded S-parameters.

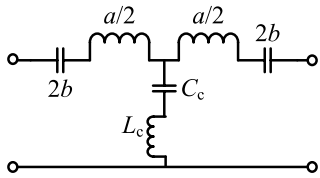

Figure 10. Circuit model of the unit cell without parallel inductors.

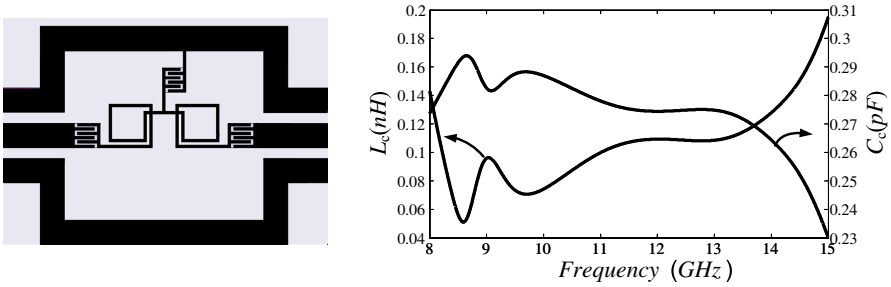

(a) (b)

Figure 11. (a) T-model structure. (b) Diagrams of L_c and C_c.

Figure 11 presents the T-model structure and the diagrams of L_c and C_c. L_c and C_c are found to be equal to 0.1 nH and 0.28 pF, respectively, at the frequency of 11.45 GHz.

3.6.2. Parallel Spiral Inductors

Due to proximity of parallel spiral inductors with ground strips and therefore coupling with it, the parallel spiral inductors are modelled with a parallel inductor (L_{2d}) and parallel capacitor (C_{2d}) in which the quantity $2d = 1.18$ nH is related to the equivalent inductance by:

$$\frac{1}{j\omega 2d} = j\omega C_{2d} + \frac{1}{j\omega L_{2d}} \tag{12}$$

To determine L_{2d} and C_{2d}, the parallel IDC of the unit cell is removed from the configuration, which results in a Π-model (Fig. 12). In this structure, L_{2d} and C_{2d} are determined from Y-parameters as:

$$\begin{aligned} L_{2d} &= \frac{2}{j\omega}\frac{1}{Y_{11d} + Y_{12d} - \omega\frac{d}{d\omega}(Y_{11d} + Y_{12d})} \\ C_{2d} &= \frac{1}{j2\omega}\left(Y_{11d} + Y_{12d} + \omega\frac{d}{d\omega}(Y_{11d} + Y_{12d})\right) \end{aligned} \tag{13}$$

Fig. 13 presents the Π-model structure and the diagrams of L_{2d} and C_{2d}. L_{2d} and C_{2d} are found to be equal to 1.01 nH and 0.027 pF, respectively, at the frequency of 11.45 GHz.

Using L_c and C_c instead c and L_{2d} and C_{2d} instead $2d$, new parameters, called set II, are obtained and given in Table 2. The results of using these parameters in the circuit model are also depicted in Figs. 9(b) and (c) which shows acceptable agreement although with a discrepancy which may be due to the not considering the coupling between the elements and also the loss of the elements.

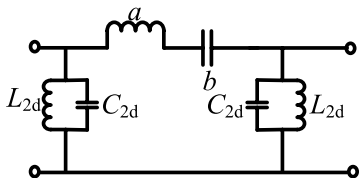

Figure 12. Circuit model of the unit cell without parallel IDC.

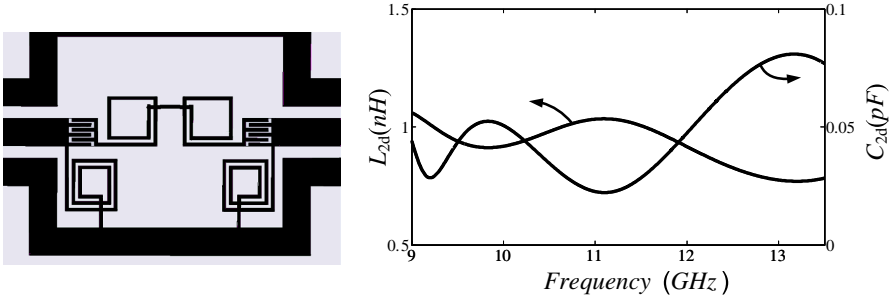

(a) (b)

Figure 13. (a) Π-model structure. (b) Diagrams of L_{2d} and C_{2d}.

4. CONCLUSION

The parameters of designed unit cell were obtained in the balanced condition with Bloch impedance of equal to 50 Ω. For tuned capacitor and inductor, ferroelectric IDC and spiral inductor were used. Initially, the individual elements of the unit cell, were simulated and their dimensions were varied until the desired values were achieved. Then, they were connected together to form a Π-model structure, and once again their dimensions were varied to reach the desired values. Finally, to complete the unit cell, the shunt capacitor was added and its length was varied so that the balanced condition was obtained. taking into account the parasitic elements of the parallel elements, the parallel IDC was modelled with a series capacitor and inductor and their values were obtained in T-model configuration of the unit cell and the parallel spiral inductors were modelled with a parallel inductor and capacitor and their values were obtained in Π-model configuration of the unit cell. Using these values, new parameters called set II were obtained and the results of using parameters set II were compared to simulation results which revealed a little discrepancy which was related to not considering the coupling between the elements and also the loss of the elements.

REFERENCES

1. Caloz, C., T. Itoh, and A. Rennings, "CRLH metamaterial leaky-wave and resonant antennas," *IEEE Antennas and Propagation Magazine*, Vol. 50, No. 5, 25–39, Oct. 2008.
2. Yu, A., F. Yang, and A. Z. Elsherbeni, "A dual band circularly polarized ring antenna based on composite right and left handed metamaterials," *Progress In Electromagnetics Research*, Vol. 78, 73–81, 2008.
3. Abdelaziz, A. F., T. M. Abuelfadl, and O. L. Elsayed, "Realization of composite right/left-handed transmission line using coupled lines," *Progress In Electromagnetics Research*, Vol. 92, 299–315, 2009.
4. Camacho-Peñalosa, C., T. M. Martín-Guerrero, J. Esteban, and J. E. Page, "Derivation and general properties of artifitial lossless balanced composite right/left-handed transmission line of arbitrary order," *Progress In Electromagnetics Research B*, Vol. 13, 151–169, 2009.
5. Sánchez-Martínez, J. J., E. Márquez-Segura, P. Otero, and C. Camacho-Peñalosa, "Artifitial transmission line with left/right-handed behaviour based on wire bonded interdigital capacitor," *Progress In Electromagnetics Research B*, Vol. 11, 245–264, 2009.
6. Upadhyay, D. K. and S. Pal, "Design of novel improved unit cell for composite right/left-handed transmission line based microwave circuits," *International Journal of Engineering Science and Technology (IJEST)*, Vol. 3, No. 6, 4962–4967, 2011.
7. Lin, S., "Composite right/left-handed band-pass filters with wide fractional bandwidth based on dual-metal-plane structure," *Microw. Opt. Technol. Letter*, Vol. 52, 1810–1813, 2010.
8. Dong, Y. and T. Itoh, "Composite right/left-handed substrate integrated waveguide and half mode substrate integrated waveguide leaky-wave structures," *IEEE Trans. on Antennas and Propagation*, Vol. 59, No. 3, 767–775, Mar. 2011.
9. Lim, S., C. Caloz, and T. Itoh, "Metamaterial-based electronically controlled transmission-line structure as a novel leaky-wave antenna with tunable radiation angle and beamwidth," *IEEE Trans. on Microw. Theory and Tech.*, Vol. 53, No. 1, 161–173, Jan. 2005.
10. Abdalla, M., K. Phang and G. V. Eleftheriades, "A planar electronically steerable patch array using tunable PRI/NRI phase shifters," *IEEE Trans. on Microw. Theory and Tech.*, Vol. 57, No. 3, 531–541, Mar. 2009.

11. Caloz, C. and T. Itoh, *Electromagnetic Metamaterials: Transmission Line Theory and Microwave Applications*, John Wiley and Sons Inc., 2006.
12. Bahl, I., *Lumped Elements for RF and Microwave Circuits*, Artech House Inc., 2003.
13. Nath, J., D. Ghosh, J. Maria, A. I. Kingon, W. Fathelbab, P. D. Franzon, and M. B. Steer, "An electronically tunable microstrip bandpass filter using thin-film barium strontium titanate (BST) varactors," *IEEE Trans. on Microw. Theory and Tech.*, Vol. 53, No. 9, 2707–2711, Sep. 2005.
14. Tong, W., Z. Hu, H. Zhang, C. Caloz, and A. Rennings, "Study and realisation of dual-composite right/left-handed coplanar waveguide metamaterial in MMIC technology," *IET Microwaves, Antennas and Propagation*, Vol. 2, No. 7, 731–736, 2008.
15. Edwards, T. C. and M. B. Steer, *Foundations of Interconnect and Microstrip Design*, 3rd edition, John Wiley and Sons Inc., 2000.
16. Pozar, D. M., *Microwave Engineering*, 3rd edition, John Wiley and Sons Inc., 2005.
17. Volakis, J. L., *Antenna Engineering Handbook*, 4th edition, McGraw-Hill Co., 2007.
18. Gevorgian, S., T. Martinsson, L. J. P. Linnér, and E. L. Kollberg, "CAD models for multilayered substrate interdigital capacitors," *IEEE Trans. on Microw. Theory and Tech.*, Vol. 44, No. 6, 896–904, Jun. 1996.